Triplet Excited States of Some Thiophene and Triazole Substituted Platinum(II) Acetylide Chromophores

Eirik Glimsdal,*,† Ingunn Dragland,† Marcus Carlsson,‡ Bertil Eliasson,‡ Thor Bernt Melø,† and Mikael Lindgren†

Department of Physics, Norwegian University of Science and Technology, NO-7491 Trondheim, Norway, and Department of Chemistry, Umeå University, SE-901 87 Umeå, Sweden

Received: September 19, 2008; Revised Manuscript Received: January 21, 2009

The photophysical properties of a series of platinum(II) acetylide compounds (*trans*-$Pt(PBu_3)_2(C{\equiv}C\text{-}R)_2$) with the R group consisting of two or three aryl rings (phenyl, phenyl/thiophenyl, phenyl/triazolyl) linked together with ethynyl groups were systematically investigated. Four new structurally similar compounds are reported with: (i) a bithiophene unit in the ligands, (ii) methyl or (iii) methoxy substituents on the aryl ring ligands that promote a more twisted conformation along the long axis of the molecule, and (iv) with two different alkynylaryl ligands giving rise to an asymmetric substitution with respect to the photoactive metal ion center. The spectroscopic studies include optical absorption, spectrally and time-resolved luminescence, as well as transient absorption spectra. The ground-state UV absorption between 300 and 420 nm gave rise to fluorescence with quantum efficiencies in the range of 0.1−1% and efficient intersystem crossing to triplet states. Phosphorescence decay times were in the order of 10−500 μs in oxygen-evacuated samples. The triplet states also lead to strong broadband triplet−triplet absorption between 400 and 800 nm. The complex with asymmetric substitution was found to populate two triplet states of different structure and energy.

1. Introduction

Although the focus of most work in the field of organic "soft" materials for nonlinear optics (NLO) has been on all-organic molecules, there is increasing interest in the properties and applications of organometallic systems that feature transition metals which interact strongly with a π-conjugated electronic system. This can result in both efficient intersystem crossing (ISC) to long-lived excited states[1] resulting in a variety of nonlinear absorption and other photochemical processes via interaction between light and the excited-state configuration.[2,3] When engineered for a targeted application, such materials have potential use in, e.g., optical communication and data storage,[4] photovoltaic devices and lasers,[5,6] laser-protecting materials,[7−9] as well as multiphoton excitation materials for, e.g., biosensing and imaging.[10−12] A class of compounds that has attracted attention for their multiphoton absorption processes is transition metal acetylides.[13,14] The rigidity and linear geometry of the alkynyl groups make them an attractive system for the design of photon-controlling molecular units. Such organometallic complexes can show extraordinary photophysical properties due to the electronic interaction between the transition metal and the organic molecular framework with an extended π-electron delocalization.[15,16] Some reviews of NLO properties of organometallic and coordination complexes have been published,[17,18] together with some more specific reviews of metallic alkynyl complexes.[13,14]

Metals such as Re, Ru, Ir, Pt, Au, Ni, and Fe exert a strong influence on the optical properties of a conjugated system via several mechanisms, including spin−orbit coupling induced singlet−triplet mixing.[1,19] Organometallic complexes can have efficient single- and multiphoton absorption and short response times for absorption from triplet states. In addition, stable complexes can be prepared for ease of fabrication and may be suitable for integration into composites as well as for providing a larger flexibility in the design state than that of regular organic systems.[4] Variation in metal, oxidation state, ligand environment, and geometry can potentially permit photoresponses to be tuned in ways not possible for purely organic compounds.

Although different heavy metals can be incorporated in conjugated complexes, the platinum atom may be preferred when colorless chromophores are required. For example, square planar *trans*-$(PEt_3)_2Pt(CC\text{-}Ph)_2$ has the absorption maximum of its longest wavelength band at 328 nm.[20] Over the last several years, square planar platinum(II) acetylides, e.g., bis((4-(phenylethynyl)phenyl)ethynyl)bis(tri-*n*-butylphosphine)platinum(II), abbreviated **Pt1** (Figure 1), are one type of transition metal complexes that has been investigated for two-photon absorption (TPA), excited-state absorption (ESA), and OPL in high-intensity light.[7,21−24] Thus, there is a considerable interest also in the synthesis, spectroscopy, nonlinear optics, and structure-to-property relationships of similar platinum acetylides.[8,25−31]

Because Pt acetylides have high linear transmission in the visible region and significant nonlinear absorption over a wide spectral region they are potentially suitable for OPL applications.[7,8,21] The heavy atom introduces spin−orbit coupling, with efficient intersystem crossing (ISC) from the singlet to the triplet energy states. Both the absorption and lifetime of the triplet state have been found to be important for good OPL performance.[31,32] In earlier studies by the present authors the synthesis, photophysical characterization and OPL of several thiophene-[33−36] and triazole-[37,38] containing platinum acetylides were investigated; see structures **T1**−**T4**, **T6**, **T7**, and **Z1**−**Z3** in Figure 1. However, in order to explain the OPL mechanisms and performance of the different chromophores, also the triplet−triplet state absorption in the visible region is found to be essential.[32]

* To whom correspondence should be addressed. Phone: +47 735 93367. Fax: +47 735 97710. E-mail: eirik.glimsdal@ntnu.no.
† Norwegian University of Science and Technology.
‡ Umeå University.

10.1021/jp8083277 CCC: $40.75
Published on Web 03/17/2009

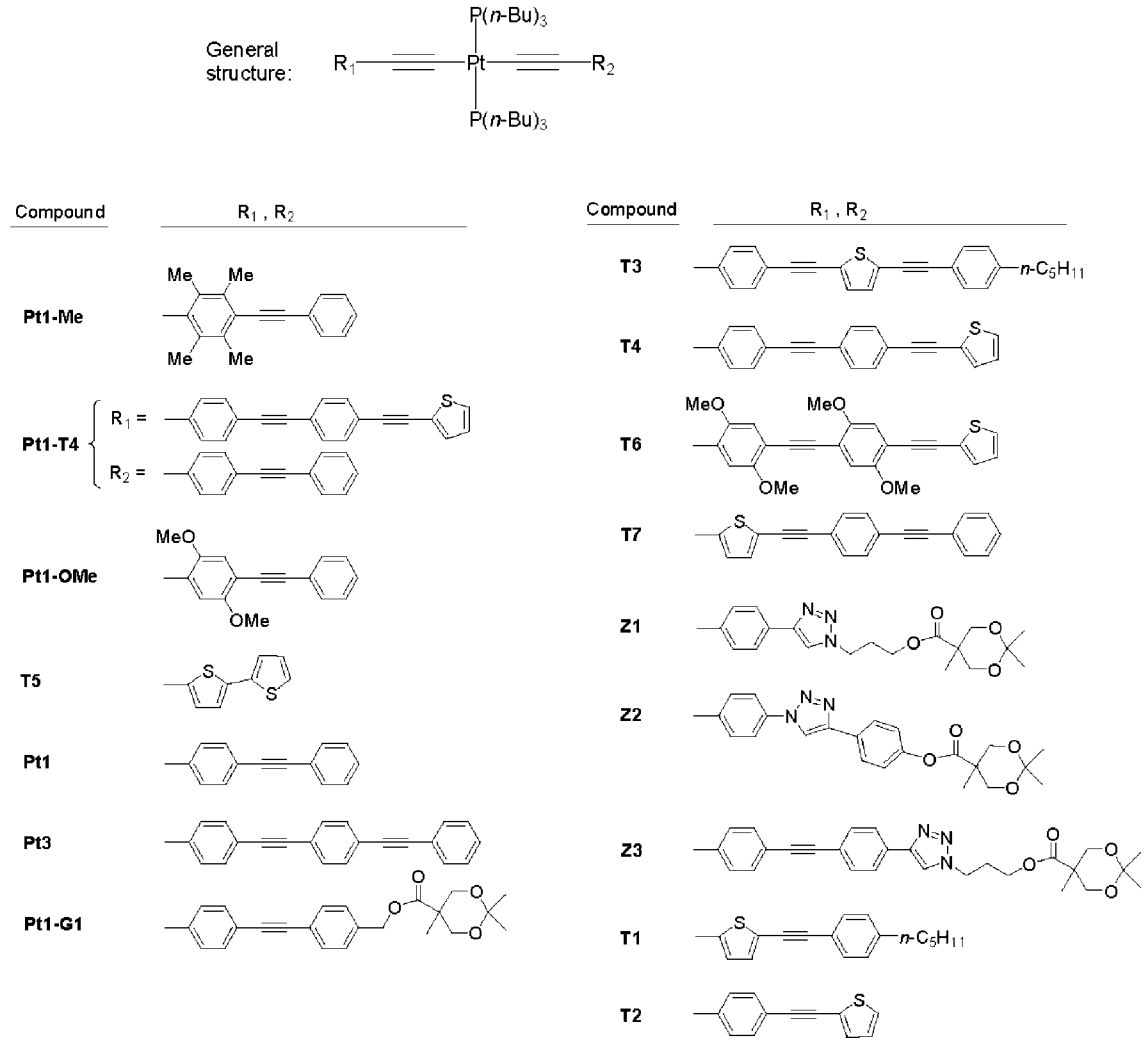

Figure 1. Structures and acronyms of Pt(II) acetylides investigated in this work.

In this study we have measured the triplet−triplet absorption (transient absorption) of a series of Pt acetylides with thiophene and triazole groups within the ligands, in tetrahydrofuran (THF) solutions. In addition to a detailed spectroscopic investigation of our previously reported molecules we here present results of four new modified Pt-acetylide chromophores, not previously investigated for their photophysical properties, structures **Pt1-Me**, **Pt1-T4**, **Pt1-OMe**, and **T5** in Figure 1. The specific ligand substitution schemes of the molecules in the new series were introduced in order to investigate certain influences of conjugation and symmetry of the organic π-electron moieties proximate to the photoactive Pt center.

2. Methodology

2.1. Sample Preparation. The synthesis of the four new chromophores, denoted **Pt1-Me**, **Pt1-T4**, **Pt1-OMe**, and **T5** (Figure 1), is described in detail in the following section. Terminal alkynes were coupled with aryl halides using Pd(II)/(Cu(I) catalysts, by similar procedures as earlier reported,[8,33] Scheme 1. The preparation of the compounds with (i) dendritic end groups (**Pt1-G** series), (ii) thiophenyl end groups (**T** series), and (iii) triazole end groups (**Z** series) were reported by Vestberg,[8] Lind[33] and Carlsson,[35] and Westlund,[37] respectively. All reactions were carried out in Ar atmosphere with dry solvents. THF and triethylamine (TEA) were distilled from potassium and potassium hydride, respectively. Reactants and reagents were obtained from Sigma-Aldrich Co. and used as received. Compounds 1,4-diiodo-2,3,5,6-tetramethylbenzene,[39] *trans*-$PtCl_2(P(n\text{-}Bu)_3)_2$,[40] 1-ethynyl-4-phenylethynyl-benzene,[41] 2-[4-(4-ethynyl-phenylethynyl)-phenylethynyl]-thiophene,[35] 4-(4-iodo-2,5-dimethoxy-phenyl)-2-methyl-but-3-yn-2-ol,[35,42,43] 1-ethynyl-2,5-dimethoxy-4-phenylethynyl-benzene (**3**),[44] 5-iodo-[2,2′]-bithiophenyl,[45,46] and 5-ethynyl-[2,2′]bithiophenyl (**5**) [47,48] were synthesized following procedures similar to those previously reported. ^{13}C NMR data for compounds **3** and **5** was not found in the literature and is therefore provided in the following synthesis section.

Microwave synthesis was performed on a Monomode reactor, the Smith Synthesizer (Personal Chemistry AB). Reaction vials were the Smith Process Vials 2.0−5.0 mL filling volume, sealed with Teflon septa and an aluminum crimp top. Flash column chromatography (eluent given in brackets) was performed on silica gel (matrix, 60 Å, 35−70 μm, Grace Amicon). ^1H, ^{13}C, and ^{31}P NMR spectra were recorded on a Bruker DRX 400 or a Bruker DRX 360. ^1H and ^{13}C chemical shifts are reported relative to the solvent $CHCl_3$ (δ_H 7.26 ppm) or $CDCl_3$ (δ_C 77.0 ppm) signals, respectively, while ^{31}P chemical shifts are given relative to external 0.1 M $P(C_6H_5)_3$ in $CDCl_3$ with $\delta = -4.89$, which corresponds to $\delta = 0$ for 85% H_3PO_4. IR spectra were recorded on an ATI Mattson Genesis Series FTIR spectrometer. Elemental analyses were performed by Mikrokemi AB, Uppsala, Sweden.

SCHEME 1: Synthesis of Pt Arylethynyl Complexes[a]

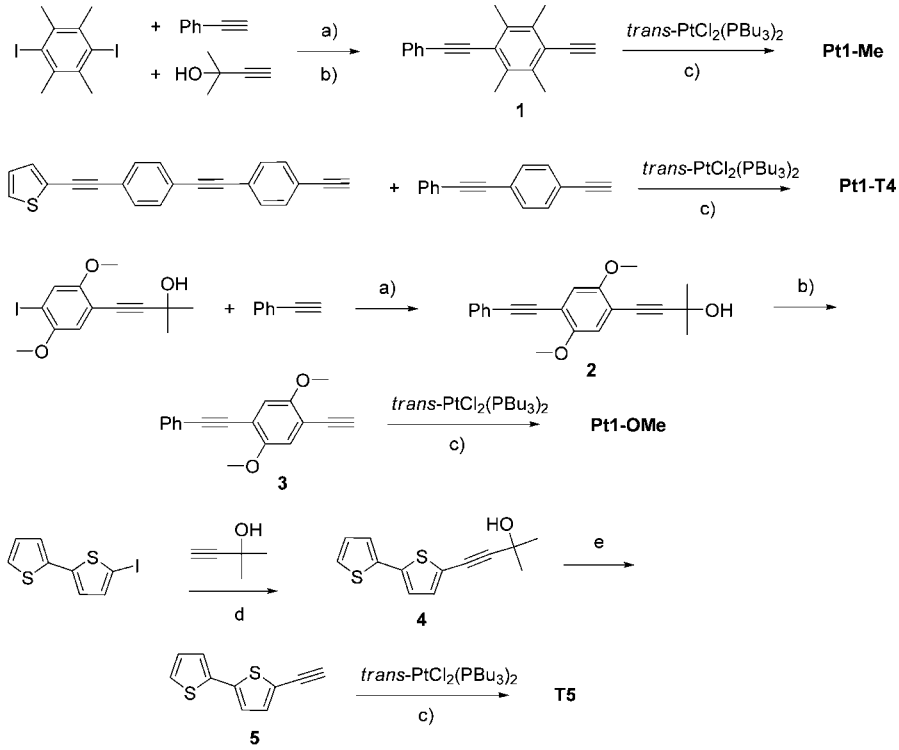

[a] (a) $PdCl_2(PPh_3)_3$, CuI, PPh_3, TEA, and THF; (b) KOH; (c) CuI, TEA, and THF; (d) $PdCl_2(PPh_3)_3$, CuI, PPh_3, TEA, and DMF; (e) KH.

The fluorophore Coumarin 110 (7-diethylamino-coumarin) from Sigma-Aldrich was used as a spectroscopic reference compound in fluorescence quantum yield measurements.[34] Dry samples were dissolved in THF (≥99.5% spectrophotometric grade, from Sigma-Aldrich) into 10-mm quartz cells (Hellma Precision). The samples were diluted to 1−50 μM depending on the type of experiment.

2.2. Synthesis of New Compounds. ***1-Ethynyl-2,3,5,6-tetramethyl-4-(phenylethynyl)benzene,*** **1.** 1,4-Diiodo-2,3,5,6-tetramethylbenzene (4.54 g, 11.8 mmol), $PdCl_2(PPh_3)_2$ (0.187 g, 0.268 mmol), PPh_3 (70 mg, 0.268 mmol), and CuI (100 mg, 0.535 mmol) were dissolved in THF (10 mL) and TEA (10 mL). 2-Methylbut-3-yn-2-ol (1.04 mL, 10.7 mmol) was added, and the solution was stirred at room temperature. After 30 min, phenylacetylene (1.8 mL, 16 mmol) was added, and the reaction was stirred at 70 °C for 24 h. The resulting mixture was diluted with $CHCl_3$ and washed twice with 1 M HCl(aq). The organic extract was dried with anhydrous $MgSO_4$, filtered, and concentrated. The residue was mixed with hexane and filtered. The filtrate was dissolved in toluene (200 mL), and KOH (0.56 g, 10 mmol) was added. The solution was refluxed for 3.5 h and cooled to room temperature. After removal of the solvent the residue was dissolved in $CHCl_3$ and washed with 1 M HCl(aq). The organic extract was dried with anhydrous $MgSO_4$, filtered, and concentrated. Flash chromatography over silica [20:1 heptane:EtOAc] gave 0.78 g (3.0 mmol) as a colorless solid in 28% overall yield; ^{1}H NMR (360 MHz, $CDCl_3$) δ 7.67−7.54 (m, 2 H), 7.45−7.32 (m, 3 H), 3.59 (s, 1 H), 2.52 (s, 6 H), 2.48 (s, 6 H); ^{13}C NMR (91 MHz, $CDCl_3$) δ 136.2, 135.6, 131.3, 128.3, 128.1, 123.7, 123.6, 122.1, 98.0, 88.4, 85.6, 82.5, 18.3, 18.2.

trans-Di-[4-(phenylethynyl)-2,3,5,6-tetramethyl-phenylethynyl]-bis-(tri-n-butylphosphine)-platinum(II), **Pt1-Me.** Alkyne **1** (50 mg, 0.19 mmol) and *trans*-$PtCl_2(P(n\text{-}Bu)_3)_2$ (62 mg, 0.092 mmol) were dissolved in THF (2 mL) and TEA (2 mL). To the solution, CuI (2 mg, 0.01 mmol) was added and heated with microwaves in a monomode instrument at 60 °C for 6 min. The resulting mixture was diluted with $CHCl_3$ and washed twice with 1 M HCl(aq). The organic extract was dried with anhydrous $MgSO_4$, filtered, and concentrated. Flash chromatography over silica (20:1 heptane:EtOAc) followed by recrystallization from $CHCl_3$/MeOH (an orange solid precipitated first, which was removed by filtration) gave colorless crystals, 26 mg (25% yield). After a prolonged time an additional 61 mg of crystals was obtained from the mother liquid to give a total yield of 85%; ^{1}H NMR (360 MHz, $CDCl_3$) δ 7.60−7.52 (m, 4 H), 7.40−7.30 (m, 6 H), 2.49 (s, 12 H), 2.48 (s, 12 H), 2.16−1.97 (m, 12 H), 1.68−1.54 (m, 12 H), 1.46− 1.33 (m, 12 H), 0.90 (t, J = 7.36 Hz, 18 H); ^{13}C NMR (91 MHz, $CDCl_3$) δ 135.0, 134.0, 131.2, 129.4, 128.3, 127.6, 124.4, 119.2 (apparent triplet), 119.1, 108.1, 96.4, 89.6, 26.5, 24.4 (apparent triplet), 24.0 (apparent triplet), 18.7, 19.6, 13.9. Anal. Calcd for $C_{64}H_{88}P_2Pt$: C, 68,98; H, 7,96. Found: C, 68.9; H, 8.0.

trans-[4-(Phenylethynyl)-phenylethynyl]-[4-(4-(2-thiophenyl-ethynyl)-phenylethynyl)-phenylethynyl]-bis(tributylphosphine)-platinum(II), **Pt1-T4.** 1-Ethynyl-4-phenylethynyl-benzene (90 mg, 0.11 mmol), 2-[4-(4-ethynyl-phenylethynyl)-phenylethynyl]-thiophene (36 mg, 0.12 mmol), and *trans*-$PtCl_2(P(n\text{-}Bu)_3)_2$ (40 mg, 0.060 mmol) were dissolved in a solution of THF (2 mL) and TEA (2 mL). The solution was heated to 60 °C, and CuI (1.5 mg, 0.008 mmol) was added. After 6 min the solution was allowed to reach room temperature, and the resulting mixture was diluted with $CHCl_3$. The organic solution was washed with 1 M HCl(aq), dried with anhydrous $MgSO_4$, filtered, and concentrated. The residue was crystallized from $CHCl_3$/hexane and filtered. After concentration of the filtrate and recrystallization from EtOH/$CHCl_3$, 89 mg (0.080 mmol) of slightly yellow crystals were obtained (75% yield); ^{1}H NMR (360 MHz, $CDCl_3$) δ 7.54−7.46 (m, 6 H), 7.41−7.28 (m, 9 H), 7.26−7.21 (m, 4 H), 7.02 (dd, J_1 = 5.0 Hz, J_2 = 3.8 Hz, 1 H), 2.19- 2.07

(m, 12 H), 1.68−1.56 (m, 12 H), 1.52−1.39 (m, 12 H), 0.93 (t, $J = 7.2$ Hz, 18 H); ^{13}C NMR (91 MHz, $CDCl_3$) δ 132.1, 131.5, 131.4, 131.4. 131.2, 131.2, 130.7, 129.3, 129.0, 128.3, 128.0, 127.5, 127.2, 123.5, 123.1, 122.4, 119.2, 118.9, 112.2 (apparent triplet), 111.7 (apparent triplet), 109.3, 92.8, 92.1, 90.0, 89.8, 89.5, 84.4, 26.3, 24.4 (apparent triplet), 23.9 (apparent triplet), 13.8; ^{31}P NMR (146 MHz, $CDCl_3$) δ 3.84 ($J_{P-Pt} = 2343$ Hz). Anal. Calcd for $C_{62}H_{74}P_2PtS$: C, 67.19; H, 6.73. Found: C, 66.7; H, 6.6.

***4-(2,5-Dimethoxy-4-phenylethynyl-phenyl)-2-methyl-but-3-yn-2-ol,* 2.** To a mixture of THF (8 mL) and TEA (8 mL) was added 4-(4-iodo-2,5-dimethoxy-phenyl)-2-methyl-but-3-yn-2-ol (0.615 g, 1.77 mmol), CuI (17 mg, 0.088 mmol), PPh_3 (12 mg, 0.044 mmol), and $PdCl_2(PPh_3)_2$ (31 mg, 0.044 mmol). Subsequently, ethynylbenzene (0.27 g, 2.7 mmol) was added to the solution, and the reaction was stirred at 60 °C for 1 h. The resulting mixture was diluted with $CHCl_3$ and washed twice with 1 M HCl(aq). The organic extract was dried with anhydrous $MgSO_4$, filtered, and concentrated. Flash chromatography over silica (2:1 heptane:EtOAc) gave a light-yellow solid (0.559 g, 1.74 mmol) in 98% yield; ^{1}H NMR (400 MHz, $CDCl_3$) δ 7.59−7.52 (m, 2 H), 7.37−7.31 (m, 3 H), 6.99 (s, 1H), 6.92 (s, 1H), 3.87 (s, 3 H), 3.85 (s, 3 H), 2.35 (broad s, 1H), 1.64 (s, 6 H); ^{13}C NMR (100 MHz, $CDCl_3$) δ 153.8, 153.8, 131.7, 128.4, 128.3, 123.1, 115.8, 115.7, 113.3, 112.8, 99.5, 94.9, 85.5, 78.3, 65.7, 56.4, 56.4 31.4.

***1-Ethynyl-2,5-dimethoxy-4-phenylethynyl-benzene,* 3.** Compound **2** was deprotected using KOH in toluene. ^{1}H NMR (400 MHz, $CDCl_3$) data were in agreement with that in a previous work.[44] ^{13}C NMR (100 MHz, $CDCl_3$) δ 154.3, 153.6, 131.5, 128.3, 128.2, 122.2, 116.1, 115.4, 113.9, 111.7, 95.0, 85.3, 82.6, 79.8, 56.2, 56.2.

***trans-Di-[2,5-dimethoxy-4-(phenylethynyl)-phenylethynyl]-bis-(tri-n-butylphosphine)-platinum(II),* Pt1-OMe.** *trans*-$PtCl_2(P(n\text{-}Bu)_3)_2$ (0.256 g, 0.381 mmol) and alkyne **3** (0.200 g, 0.763 mmol) were dissolved in TEA (3 mL) and THF (4 mL) and heated to 60 °C. CuI (1.5 mg, 0.008 mmol) was added and the reaction was stirred for an additional 5 min. The resulting mixture was allowed to reach room temperature and diluted with $CHCl_3$. The organic solution was washed twice with 1 M HCl(aq), dried with anhydrous $MgSO_4$, filtered, and concentrated. Flash chromatography over silica (10:1 heptane:EtOAc) gave an orange-yellow solid (0.368 g, 0.328 mmol) in 86% yield; ^{1}H NMR (400 MHz, $CDCl_3$) δ 7.57−7.53 (m, 4 H), 7.36−7.28 (m, 6 H), 6.91 (s, 2 H), 6.83 (s, 2 H), 3.85 (s, 3 H), 3.79 (s, 3 H), 2.28−2.16 (m, 12 H), 1.68−1.55 (m, 12 H), 1.52−1.39 (m, 12 H), 0.92 (t, $J = 7.2$ Hz, 18 H); ^{13}C NMR (100 MHz, $CDCl_3$) δ 153.8, 153.8, 131.4, 128.1, 127.8, 123.6, 119.6, 116.3 (apparent t, $J = 14.8$ Hz), 115.3, 115.0, 108.8, 105.0, 93.4, 86.5, 56.2, 55.8, 26.2, 24.3 (apparent t, $J = 7.0$ Hz), 23.5 (apparent t, $J = 17.4$ Hz), 13.8. Anal. Calcd for $C_{60}H_{80}O_4P_2Pt$: C, 64.21; H, 7.18. Found: C, 64.3; H, 7.3.

4-[2,2′]Bithiophenyl-5-yl-2-methyl-but-3-yn-2-ol, 4. 5-Iodo-[2,2′]bithiophenyl (0.156 g, 0.534 mmol), PPh_3 (1.4 mg, 5.3×10^{-6} mol), $Pd(PPh_3)_2Cl_2$ (7.5 mg, 1.1×10^{-5} mol), CuI (4.1 mg, 2.1×10^{-5} mol), 4-(4-iodo-phenyl)-but-3-yn-2-ol (53.9 mg, 0.641 mmol), DMF (1.5 mL), and TEA (1.5 mL) were mixed in a heavy-wall Smith process vial at 120 °C for 6 min in the microwave cavity. The mixture was subsequently dissolved in diethyl ether and washed three times with 1 M HCl(aq). The organic layer was dried with anhydrous $MgSO_4$, filtered, and concentrated. Flash chromatography [heptane:ethyl acetate 4:1] gave 114 mg (0.489 mmol) as yellow crystals in 86% yield: IR υ 3239, 2983, 1359, 1153, 950, 796, 686 cm^{-1}; ^{1}H NMR (400 MHz, $CDCl_3$) δ 7.21 (dd, $J_1 = 5.1$ Hz, $J_2 = 1.1$ Hz, 1H), 7.16 (dd, $J_1 = 3.6$ Hz, $J_2 = 1.1$ Hz, 1H), 7.06 (d, $J = 3.8$ Hz, 1H), 7.03−6.98 (m, 2H), 2.16 (s, 1H), 1.62 (s, 6H); ^{13}C NMR (100 MHz, $CDCl_3$) δ 138.80, 136.76, 132.93, 128.00, 125.06, 124.29, 123.42, 121.36, 98.47, 75.57, 65.90, 31.41.

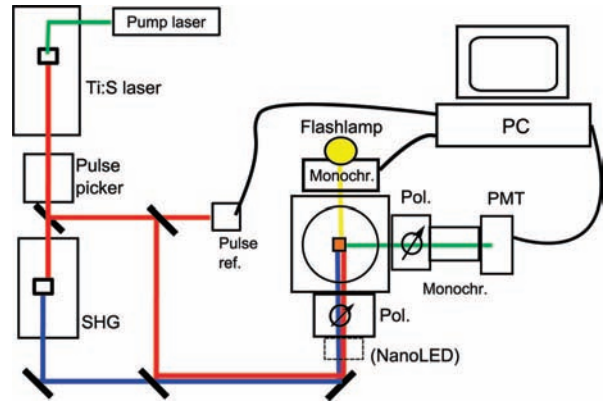

Figure 2. Schematic setup for the time-resolved and luminescence measurements. The setup can use the fundamental red laser beam, for two-photon excitation, or the blue SHG beam for one-photon excitation. See details in text. The laser excitation path can also be replaced by a NanoLED or Flash-lamp, depending on the excitation conditions required.

5-Ethynyl-[2,2′]bithiophenyl, 5. 4-[2,2′]Bithiophenyl-5-yl-2-methyl-but-3-yn-2-ol (0.312 g, 1.26 mmol) was dissolved in toluene (60 mL), and KH (0.101 g, 2.51 mmol) was added. The reaction mixture was refluxed until all starting material had reacted (30 min) and then quenched with water. The resulting mixture was washed two times with brine and the organic extract was dried with $MgSO_4$, filtered, and concentrated. Flash chromatography [heptane] gave 0.150 g 0.789 mmol) as an oil in 63% yield; IR υ 3288, 3070, 2919, 2098, 1452, 1423, 1201, 768, 696 cm^{-1}; ^{1}H NMR (400 MHz, $CDCl_3$) δ 7.24 (dd, $J_1 = 5.1$ Hz, $J_2 = 1.1$ Hz, 1H), 7.20−7.17 (m, 2H), 7.04−7.01 (m, 2H), 3.40 (s, 1H); ^{13}C NMR (100 MHz, CDCl3) δ 139.29, 136.56, 134.00, 128.3, 125.26, 124.52, 123.34, 120.66.

trans-Di-([2,2′]bithiophenyl-ethynyl)-bis-(triphenylphosphine)-platinum(II), T5. 5-Ethynyl-[2,2′]bithiophenyl (0.090 g, 0.473 mmol), *trans*-$PtCl_2(P(n\text{-}Bu)_3)_2$ (0.150 g, 0.235 mmol), TEA (2 mL), THF (2 mL), and CuI (4 mg, 0.02 mmol) were mixed in a heavy-wall Smith process vial at 60 °C for 4 min in the microwave cavity. The mixture was subsequently dissolved in $CHCl_3$ and washed two times with 1 M HCl(aq). The organic layer was dried with anhydrous $MgSO_4$, filtered, and concentrated. Flash chromatography [heptane:ethyl acetate 13:1] gave 0.213 g (0.218 mmol) as yellow crystals in 97% yield; ^{1}H NMR (400 MHz, $CDCl_3$) δ 7.15 (dd, $J_1 = 5.1$ Hz, $J_2 = 1.2$ Hz, 2H), 7.08 (dd, $J_1 = 3.6$ Hz, $J_2 = 1.2$ Hz, 2H), 6.98 (dd, $J_1 = 5.1$ Hz, $J_2 = 3.6$ Hz, 2H), 6.94 (d, $J = 3.7$ Hz, 2H), 6.73 (d, $J = 3.7$ Hz, 2H), 2.15−2.07 (m, 12H), 1.65−1.55 (m, 12H), 1.53−1.42 (m, 12H), 0.95 (t, $J = 7.2$, 18H). Anal. Calcd for $C_{44}H_{64}P_2PtS_4$: C, 54.02; H, 6.59. Found: C, 53.9; H, 6.6.

2.3. Spectroscopic Characterization. Measurements of steady state optical absorption spectra were recorded for 10 μM solutions using a Shimadzu UV-1601PC spectrometer. The experimental setup for luminescence and time-resolved measurements is shown in Figure 2. A 200 fs pulsed Ti:Sapphire laser (Coherent MIRA 900-F) was used as radiation source. A pulse picker (Coherent 9200 Pulse Picker) is placed after the laser (76 MHz) to reduce and control the pulse repetition frequency (prf) between 9 kHz and 4.75 MHz. Unless otherwise stated the pulse repetition frequency used was 4.75 MHz. As

time and spectrally resolved detection unit, a Jobin Yvon IBH FluoroCube photon-counting spectrometer was used.

Fluorescence and phosphorescence decay times shorter than approximately 500 ns was measured using the system in time-correlated single photon counting (TC-SPC) mode, with a time resolution down to 0.014 ns. Longer triplet decay times were measured using the multichannel scaling mode (MCS), with a time resolution down to 500 ns per channel. The IBH TB−01 module (optical trigger) was used as a time reference using a thin glass wedge to take out a small part of the fundamental. For the single photon excitation luminescence and time-resolved measurements the fundamental laser beam was frequency doubled using a SHG crystal (Inrad Ultrafast Harmonic Generation System, Model 5−050). Steady state emission was recorded by scanning the monochromator in front of the PMT for a given pulse repetition frequency. The Ti:Sapphire laser was replaced by a NanoLED excitation source at 337 nm with 1 MHz prf, in some of the luminescence experiments. When using the MCS mode to measure long phosphorescence lifetimes (>10 μs), a white flashlamp at 20 Hz was used as excitation source (Figure 2). A monochromator was used to select the desired excitation wavelength. Fluorescence quantum yields were calculated from absorption and fluorescence measurements at five different concentrations. The absorbance at the excitation wavelength and the corrected integrated fluorescence is collected at each concentration. The relative quantum yield of two samples is then calculated from the equation given by Williams et al.[49] Using a reference sample with known quantum yield, the absolute quantum yield of the new sample can be found. A more detailed description of the procedure and experimental considerations are given in "A Guide to Recording Fluorescence Quantum Yields" from Jobin Yvon.[50] A Gaussian peak fit analysis of the absorption spectra was performed with Fityk, version 0.8.2, software.

2.4. Deoxygenation of Solutions. It is well-known that removal of oxygen/air from samples can significantly prolong the lifetimes of excited triplet states. An enhancement of the phosphorescence part of the total emission due to reduced or eliminated oxygen quenching has been shown for instance for **Pt1-G1** (Figure 1) and closely related Pt complexes.[31] The degassing of the samples resulted in a three orders-of-magnitude increment of the phosphorescence decay times. In this work, air was removed from the samples by six freeze−pump−thaw cycles using a high-vacuum pump ($\sim 10^{-4}$ Torr). The setup has been extended with an efficient turbo-pump (Varian, Model NW40 H/O) in comparison with our previous reports.[31] The samples were placed in 10-mm quartz cells (Hellma Precision) with custom-made glass vacuum-line connections with closing valves. Because the measurement cells were custom-made to fit the vacuum line, the cell could be directly put into the measurement setup after vacuum pumping, without subsequent transferring the sample to another cell. No air leakage through the valve was detected even several days after degassing.

2.5. Transient Absorption Spectroscopy. A compact flash photolysis equipment, composed of commercial and purpose-built units, was used in this investigation. A schematic setup is shown in Figure 3. In the setup, the pump beam is generated by discharging a capacitor (of capacitance $C = 2$ μF) through a linear flash-lamp (EG&G Model FXQ 269-1). The energy ($E = [^1/_2]CV^2$) of each flash (of ca. 5 μs duration) is set by applying a voltage V of 3 kV. Only a part of the electrical energy is actually converted into light by this procedure and only a fraction (amounting to ca. 10 mJ) of the emitted light falls upon the sample after passing through a pair of lenses. A part of the pump flash is picked up by a photomultiplier, whose output signal is detected via a delay generator (Princeton Instruments, Model PG200) and a digital oscilloscope (LeCroy 9410). The delayed signal (after a variable preset delay) triggers the probe lamp (EG&G Model FX-409U) which has a duration of about 2 μs. The probe light, transmitting the sample at a right angle with respect to the pump beam, is made to pass through the front portion of the sample (where the excited-state population has the largest density) and is collected, after its emergence from the sample cell, by an optical fiber to an optical multichannel analyzer (OMA) (Zeiss, MCS 224) controlled by a computer using a homemade software. The time resolution of the system is determined by the temporal width of the probe flash. The sensing elements receive not only the probe light but also a fraction of the fluorescence and phosphorescence provoked by the pump source. This induced emission therefore has to be corrected for in the transmission spectrum (more below).

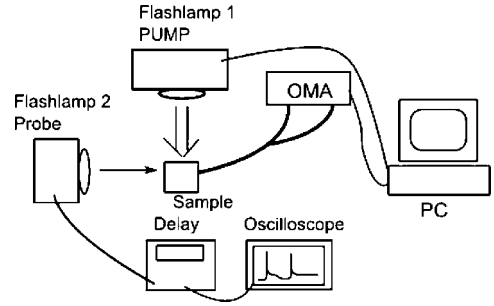

Figure 3. Schematic setup of the transient absorption (triplet−triplet) measurement. Flash-lamp 1 (pump) excites the sample. The probe light (flash-lamp 2) hits the sample at 90 degrees angle, with a specified delay controlled by the delay box. The actual flash time difference can be observed on the oscilloscope. Homemade computer software controls the flashes and the readings from the OMA. (Not all wiring is shown in the drawing.)

For data analysis, four spectral data files, each containing the reading of 1024 diodes from the OMA, are collected for constructing a single transmission difference spectrum. The dark count of the ith diode is denoted as D_i, the emission count (intensity of the luminescence emitted by the sample) as E_i, the reference count (the sum of the dark count and the signal from the probe beam after it has traversed a sample unirradiated by the pump source) as R_i, and the sample count (the sum of the dark count, the emission count and the signal representing the intensity of the probe beam after it has traversed a sample irradiated by the pump source) as S_i. The dark file is collected without firing any flash, the emission file by firing only the pump flash, the reference file by firing the probe flash alone, and the sample file by firing first the pump flash and then, after a preset delay t, the probe flash. The change in absorbance is then determined by the formula

$$\Delta A(\lambda_i,t) = \log[(R_i - D_i)/(S_i - E_i)] \qquad (1)$$

where λ_i is the wavelength of light falling on the ith diode. $\Delta A(\lambda,t)$ now becomes the transient absorption spectrum at time delay t.

The transient absorption spectrum $\Delta A(\lambda,t)$ is the change in absorption of a sample when it is struck by the pump flash (at time $t = 0$) followed by the absorption measurement taken at time t. The ground-state absorption (taken at some time $t < 0$) is given by $A_g(\lambda) = \epsilon_g(\lambda)CL$, where C is the sample concentration (initially all in the ground state) and L the sample length (here 10 mm). The absorption at time t after the pump light is

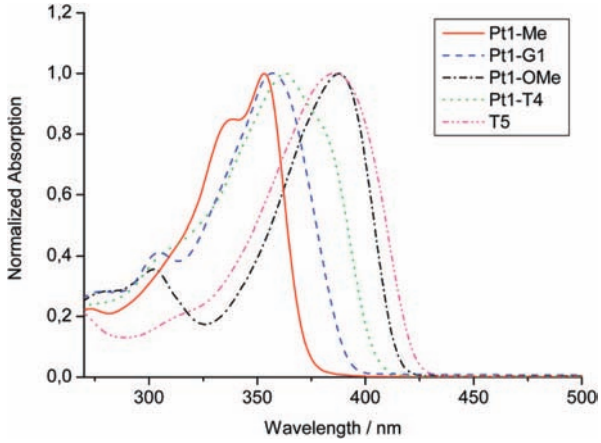

Figure 4. Normalized absorption spectra of **Pt1-Me**, **Pt1-G1**, **Pt1-T4, Pt1-OMe**, and **T5**.

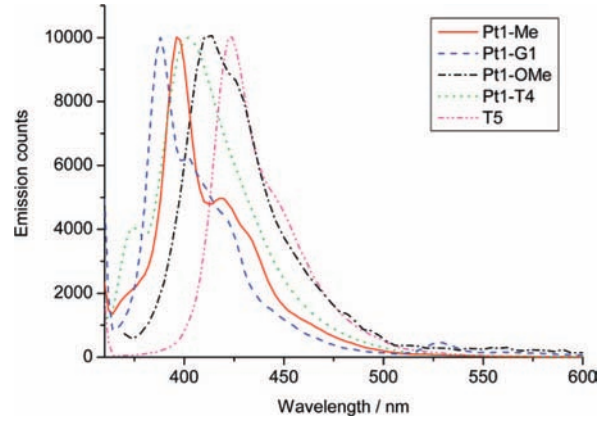

Figure 5. Normalized emission spectra for (from left to right) **Pt1-G1**, **Pt1-Me**, **Pt1-T4**, **Pt1-OMe**, and **T5**, following exciting at 360 nm. **Pt1-G1** shows a small phosphorescence peak around 525 nm.

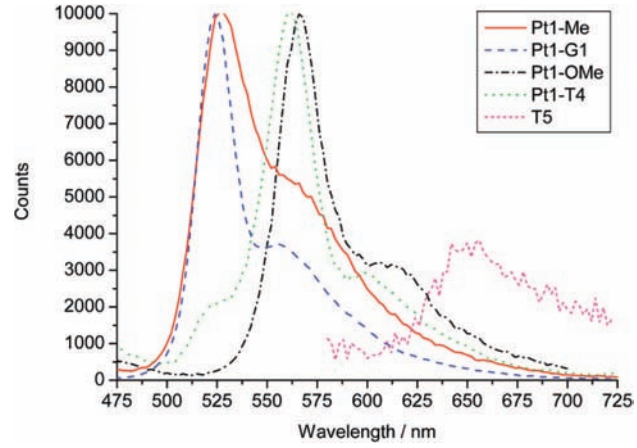

Figure 6. Normalized phosphorescence emission spectra for (from left to right) **Pt1-G1, Pt1-Me**, **Pt1-T4, Pt1-OMe**, and **T5** after degassing the samples.

given by $A(\lambda,t) = \epsilon^{T}(\lambda)C^{T}L + \epsilon(\lambda)(C - C^{T})L$; that is, absorption by the excited molecules with concentration C^{T} added to the absorption by the molecules still remaining in the ground state. The transient absorption then becomes

$$\Delta A(\lambda, t) = A(\lambda, t) - A_g(\lambda) = (\varepsilon^{T}(\lambda) - \varepsilon(\lambda))C^{T}L \quad (2)$$

The reconstruction of the true triplet−triplet absorption spectrum $A^{T}(\lambda,t)$ is finally carried out by adding a specific amount of ground-state absorption to $\Delta A(\lambda,t)$, corresponding to the amount of molecules removed from the ground state, $\epsilon(\lambda)C^{T}L$, such that all the ground-state depletion structure is removed from the transient absorption spectrum. From this the extinction coefficient of the triplet excited state $\epsilon^{T}(\lambda)$ can be determined by comparing it to the corresponding ground-state absorption.

3. Results and Discussion

3.1. Absorption and Luminescence Measurements. The previous absorption and luminescence studies of the thiophene series (**T1-T4**, **T6**, and **T7**)[33,34] and the triazoles (**Z1**, **Z2**, and **Z3**)[36,37] also included **Pt1** and **Pt1-G1**[31] for reference purposes. The four new compounds, **Pt1-Me**, **Pt1-OMe**, **Pt1-T4**, and **T5** were prepared for OPL and photophysical studies, with the aim to further investigate the nonlinear absorption mechanisms. The study of **T1**, **T2**, and **Pt1/Pt1-G1**[33,34] indicated that **T1** had a preference for a ground-state conformation with the P−Pt−P bond axis in, or close to, the plane of the aryl rings, while **T2** and **Pt1** showed a preference for the conformation with the P−Pt−P bond axis more or less perpendicular to the plane of the aromatic rings.[33] Since the former type of conformation has a rather large LUMO coefficient at the Pt nucleus, but the latter does not, and because the lowest-energy excitation is largely characterized by a HOMO−LUMO transition for both types of conformations, the spin−orbit coupling in the S_1 state of the "planar" conformation is likely to be larger than that of the "perpendicular" one. Therefore, it can be anticipated that the former type of conformation has faster ISC from S_1 to the triplet manifold than has the latter type but also that the triplet-to-S_0 ISC may be faster for the former type of structure. A faster phosphorescence decay was indeed found for **T1** (190 ns) than for **T2** (330 ns) and **Pt1-G1** (520 ns).[33,34] It was also found that the OPL response of **T1** was comparable to that of **Pt1-G1** at 532 nm but weaker at 550 and 610 nm.[33] In view of this, **Pt1-Me** was chosen as a model compound that should have large preference for the conformation with the P−Pt−P bond axis being perpendicular to the aromatic ring plane, instead of the "planar" conformation, due to steric interaction between the phosphine butyl and aromatic ring methyl groups. A longer lifetime of the triplet state could be expected for **Pt1-Me** in comparison with other Pt complexes of similar type and with similar size of the π-system if the type of conformation would be of importance for the triplet-to-S_0 ISC process and if fast methyl group rotation would not significantly enhance the nonradiative relaxation. It has also been shown by DFT calculations of a few diarylethynyl-bisphosphine Pt(II) complexes that the dominant absorption (HOMO−LUMO mentioned above) occurs at higher energy for the "perpendicular" type of conformation than for the "planar" one.[33,51] Since the diarylethynyl Pt(II) complexes generally have the absorption bands at short wavelengths in the visible region, Pt complexes with a predominating "perpendicular" conformation, such as predicted for **Pt1-Me**, can be expected to be less colored than comparable Pt complexes where the other conformation predominates, or which may exist in significant proportions of both conformations, such as **T2**, **Pt1** and **Pt1-G1**.

The absorption spectra of the four new compounds and **Pt1-G1** are shown in Figure 4, and peak absorption wavelengths (λ_{max}) and extinction coefficients (ϵ at λ_{max}) are given in Table 1. (**Pt1** and **Pt1-G1** have virtually identical absorption spectra.[31]) Except for **Pt1-Me**, the compounds show red-shifts of the main absorption peak compared to **Pt1-G1** (357 nm). The shifts are

TABLE 1: Absorption and Fluorescence Emission Peak Values, Extinction Coefficients, and Fluorescence and Phosphorescence Lifetimes of Pt1-Me, Pt1-T4, Pt1-OMe, T5, and Pt1-G1 Measured at Their Dominant Emission Peaks

sample	λ_{max} (nm)	$\epsilon(\lambda_{max})$ ($10^4 M^{-1}cm^{-1}$)	λ_{em} (nm)	τ_{fluo} (ns)	τ_{phos} [a] (μs)
Pt1-Me	353	11.8	396	0.02 (40−60%) 0.40 (40−60%)	310
Pt1-G1	357	9.3	388	~0.01 (100%) 0.30 (~1%)	190 0.25[b]
Pt1-OMe	388	10.1	412	~0.01 (100%)	190
Pt1-T4	363	11.1	402	0.013 (47%) 0.25 (36%) 0.42 (17%)	85[c] 480[c]
T5	386	12.5	424	<0.01 [d] (100%)	11

[a] In air-evacuated samples. [b] In open air (air-saturated) solution. [c] See details in text. [d] Too short to be analyzed.

from 6 nm for **Pt1-T4** to ca. 30 nm for both **T5** and **Pt1-OMe**. The large red-shift of **T5**, fast ISC, and relatively short phosphorescence decay time (see below) may indicate a "planar" conformation of this compound. **Pt1-Me** shows on the other hand a small blue-shift of the peak (λ_{max} at 353 nm) compared to **Pt1-G1**. The trend is even more obvious for the right shoulder of the bands in Figure 4. The λ_{max} values therefore increase in the order: **Pt1-Me** < **Pt1-G1** < **Pt1-T4** < and **T5** ≈ **Pt1-OMe**. The blue-shift of **Pt1-Me** compared with **Pt1-G1** can be explained by a larger proportion of **Pt1-Me** molecules having a perpendicular conformation, in the weighted average of rotamers that contributes to the absorption band, compared with the rotamer distribution for the latter compound. The absorption red-shift of **Pt1-OMe** can be accounted for by an energy-raising effect on the occupied molecular orbitals of an unsubstituted π-system (particularly of its HOMO) that results from an interaction with the π-electron donating methoxy group. Hence, a smaller HOMO−LUMO-gap is expected in **Pt1-OMe** compared with **Pt1** or **Pt1-G1**. The same trend is observed for compound **T6** compared to **T4**.[36]

The absorption spectra for all five molecules above approximately 300 nm are found to consist of 3−4 Gaussian bands by a peak-fit analysis (data not shown). It is noticed that the main peak in the spectrum of **Pt1-T4** appears very close to λ_{max} of **Pt1-G1** and that there is a pronounced shoulder in this spectrum corresponding to λ_{max} in the **T4** spectrum.[36] This suggests that there are two independent excitations of the HOMO−LUMO type in **Pt1-T4**: one for the Pt-CC-C_6H_4-CC-C_6H_5 unit (at approximately 360 nm) and one for the Pt-CC-C_6H_4-CC-C_6H_4-CC-C_4H_3S unit (the shoulder at approximately 380 nm). An obvious consequence is that proper design of asymmetrical Pt(II) complexes can result in a larger number of absorption bands (but with weaker intensity) that cover a broader range of wavelengths compared to the absorption of symmetrical Pt(II) complexes.

The luminescence spectra of air-saturated samples in THF of **Pt1-Me**, **Pt1-G1**, **Pt1-T4, Pt1-OMe**, and **T5** are shown in Figure 5, and the corresponding emission peaks (λ_{em}) and fluorescence lifetimes (τ_{fluo}) are summarized in Table 1. These fluorescence spectra show similar red shifts of the emission bands compared with **Pt1-G1** as for the absorption spectra in Figure 4. The red shifts were found to be between 8 and 35 nm, in the order **Pt1-Me**, **Pt1-T4**, **Pt1-OMe**, and **T5**. Hence, in contrast with the absorption, **Pt1-Me** displayed a red-shifted emission compared with **Pt1-G1** and therefore also a larger Stokes shift. As stated earlier, DFT calculations have shown that the HOMO−LUMO type of excitation can occur at higher energy for the "perpendicular" type of conformation than for the "planar" one.[33,51] The calculations also showed that the two conformations can have very similar energy in the ground state. This implies that a relaxed excited-state having the "planar" geometry may be lower in energy compared to a "perpendicular" structure. The larger Stokes shift of **Pt1-Me** compared with that of **Pt1-G1** can therefore be rationalized from a larger average twist toward the 'planar' structure for the former compound, before emission takes place.

The fluorescence emission lifetimes were measured at the emission peak of all compounds; see Table 1. All new dyes showed sub-nanosecond singlet lifetimes and two-component decays. **T5** shows an extremely short fluorescence decay time, which could not be deconvoluted from the laser prompt. This lifetime is therefore believed to be shorter than 10 ps, just as the dominant short component of **Pt1-G1** estimated to be about 1−10 ps,[36] due to the time resolution of the collection system and the fast and efficient competing intersystem crossing channel.[23] **Pt1-OMe** resembles **Pt1-G1** with an overall dominating short component (~100%) at, or below, approximately 10 ps. **Pt1-Me** has two components, one at 20 ps and a second at 0.4 ns. Each of them contributes with approximately 50% essentially independent of monitoring wavelength within the emission band. When the emission lifetime of **Pt1-T4** was measured at 375 nm, a weaker short component at 40 ps (15%) and a longer component at 0.3 ns (85%) were found. As the decay was measured at longer wavelengths within the emission band, the short component became dominant, and the long component became weaker.

Fluorescence quantum efficiencies (Q_{fl}) of **Pt1-Me**, **Pt1-T4**, and **T5** were found to be in the range of 10^{-2}−10^{-3} with **Pt1-G1** at 0.001 as previously reported.[34] The value of Q_{fl} for **Pt1-OMe** was found to be closer to 0.01. The emission spectrum, for all molecules, is unchanged when the excitation wavelength is varied within the absorption band.

3.2. Phosphorescence. As can be seen in Figure 5, only **Pt1-G1** displays a weak phosphorescence peak in the open air sample. The phosphorescence lifetime was measured to be about 250 ns at 525−530 nm, close to the value previously reported.[31] As with the triazoles (**Z** series) and thiophenes (**T** series), the samples in this study were air-evacuated to remove oxygen from the solutions and to prevent efficient oxygen quenching of the triplet state.[31,36,37] All samples except **T5** showed enhanced phosphorescence emission and millisecond-range lifetimes after evacuation of air; see phosphorescence spectra in Figure 6 and experimental decay times in Table 1. The compounds showed phosphorescence red shifts compared to the peak of **Pt1-G1** (at 525 nm), similar as for the fluorescence red shifts, in the order **Pt1-Me**, **Pt1-T4**, and **Pt1-OMe**. The shift is only 3 nm for **Pt1-Me** and approximately 40 nm for **Pt1-T4** and **Pt1-OMe**, with peaks at 562 and 566 nm, respectively. All spectra have the characteristic shoulder on the long wavelength side of the main peak, which is interpreted as vibration structure in the

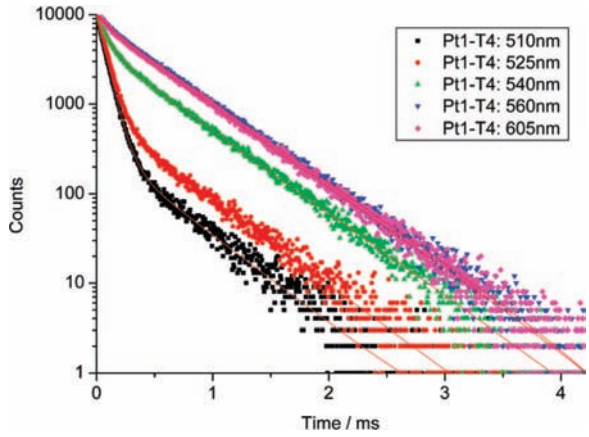

Figure 7. Phosphorescence decay traces of **Pt1-T4** at different wavelengths within the phosphorescence band. Excitation wavelength was 350 nm using the flash lamp at 20 Hz prf.

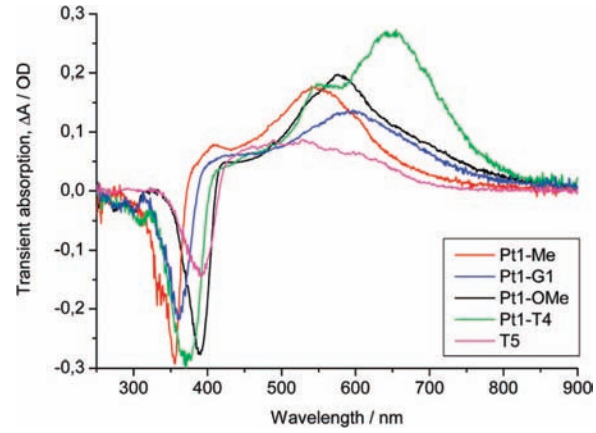

Figure 8. Transient absorption spectrum of **Pt1-Me**, **Pt1-OMe**, **Pt1-G1, Pt1-T4**, and **T5** at 250−900 nm.

TABLE 2: Phosphorescence Emission and Triplet State Absorption Peaks in the Visible Range (with Side Peaks), Degree of Ground-State Depletion, Relative Triplet-to-Ground-State Absorption, and Estimates of the Triplet Extinction Coefficient at the Absorption Peak

sample	λ_{ph} (nm)	A_{depl}	$\lambda_{triplet}$ (nm)	A_T/A_G	$\epsilon_{triplet}$ (10^4 $M^{-1}cm^{-1}$)
Pt1-Me	528	0.6	540	0.3	3.3 ± 1.1
Pt1-G1	526	0.6	596	0.3	2.9 ± 0.9
Pt1-OMe	566	0.6	575	0.45	4.5 ± 1.0
Pt1-T4	562 (525)	0.6	654 (540)	0.5	5.4 ± 1.1
T5	650	0.2	500−530	0.25	3.1 ± 1.5
T3	625	0.6	630 (525)	0.62	6.8 ± 1.1
T4	566	0.4	645 (570)	0.43	4.3 ± 1.0
T6	625	0.6	660 (570)	0.7	8.9 ± 1.2
T7	628	0.6	610	0.54	5.6 ± 1.0
Pt3	555	0.4	650 (520)	0.37	3.3 ± 0.9
Z1	486	0.07	580−620	0.3	1.5 ± 0.5
Z3	540	0.8	605	0.43	4.7 ± 1.1

emission band on the basis of studies of other Pt acetylide complexes.[51] However, it was noted that **Pt1-T4** also has a weak shoulder on the high-energy side of the main peak. This emission is coinciding with the dominating **Pt1-G1** phosphorescence around 525 nm. The main peak of **Pt1-T4** at 562 is coinciding with the peak at 566 nm of the symmetrically substituted **T4**,[36] which is discussed further below. For the **T5** compound, only a small peak at about 650 nm appears in the emission spectrum after vacuum pumping.

Phosphorescence lifetimes τ_{phos} were measured at the emission peak and at the shoulders of the main peak for all samples; see Table 1. **Pt1-G1**, **Pt1-Me, Pt1-OMe**, and **T5** were found to have the same decay time independent of the monitoring wavelength within the phosphorescence band including the vibration substructure toward the infrared side. **Pt1-G1** has a single phosphorescence decay time of 0.19 ms, which is somewhat longer than that reported earlier but still in the same order of magnitude.[31] The longer decay found here may be explained by a more efficient removal of oxygen from the sample. **Pt1-OMe** has a phosphorescence decay time being equal to that of **Pt1-G1** of 0.19 ms, while **Pt1-Me** has a longer decay time of 0.31 ms. For **T5**, the phosphorescence from 650 nm was found to have a much shorter decay time of 11 μs.

Similar to the appearance of two overlapping bands in the spectra of absorption, fluorescence, and phosphorescence of the asymmetric **Pt1-T4** molecule, the phosphorescence decay properties were found to be strikingly different than for the other compounds. Here, two different components were present in the decay trace as shown in Figure 7. At shorter wavelengths (510−540 nm), a fast decay component of 85 μs was dominating with approximately 70−80% of the total signal contribution, with a slow component of 0.48 ms contributing about 20−30%. Increasing the monitoring wavelength above approximately 540 nm, the short component gradually becomes weaker, and the slower component becomes dominating, with a contribution of 80% at 540 nm and 95% above 560 nm. It is therefore clear that the high-energy sideband found around 525 nm in the spectrum originates from a different electronic state than the main peak at 560 nm. It has previously been suggested that the first triplet state, T_1, of Pt-acetylide molecules is localized to one of the two ligands of the molecule.[29,30,51−54] The observed phosphorescence of **Pt1-T4** appears to be in agreement with this, with a superposition of emission from "**Pt1-G1**-like" phosphorescence at 525 nm and "**T4**-like" phosphorescence at 560 nm. We also note that the short-decay time component is connected to a state of higher energy than the long component. This can be explained by additional relaxation paths for the triplet state of higher energy, e.g., to the lower triplet "**T4**" state, which should reduce its total lifetime. Thus, we assign the fast decay at 525 nm to a triplet that resides on the '**Pt1** side' of **Pt1-T4** and has a fast depopulation, for example by triplet energy transfer to the "**T4**-side" of **Pt1-T4**. Consequently, the main phosphorescence peak (from the **T4** unit) displays a relatively slow decay because of a population gain from the excited "**Pt1** side". In conformity with this, we point out that compound **T4** has a phosphorescence lifetime of 0.14 ms,[35] which is significantly shorter than the 0.48 ms observed here for the triplet on the "**T4**-side" of **Pt1-T4**.

3.3. Transient Triplet−Triplet Absorption. All four new compounds showed strong triplet−triplet state absorption in the visible region (400 to 800 nm). Transient absorption spectrum for **Pt1-Me**, **Pt1-OMe**, **Pt1-T4**, **T5**, and **Pt1-G1** are shown in Figure 8. In addition, spectra of **Pt3** and several of the previously reported compounds in the **T** and **Z** series were also collected (data not shown). The wavelength data of the phosphorescence peaks (λ_{ph}), the degree of absorption depletion as a fraction of the total ground-state absorption (A_{depl}), the triplet absorption peak values in the visible range ($\lambda_{triplet}$), relative triplet-to-ground-state absorption, and estimated triplet state extinction coefficients ($\epsilon_{triplet}$) for all molecules investigated, are summarized in Table 2.

The ground-state depletion (negative peak at 350−400 nm) was estimated to be about 60% for all molecules in Figure 8 (20% for **T5**). Because of the efficient ISC, a large fraction of

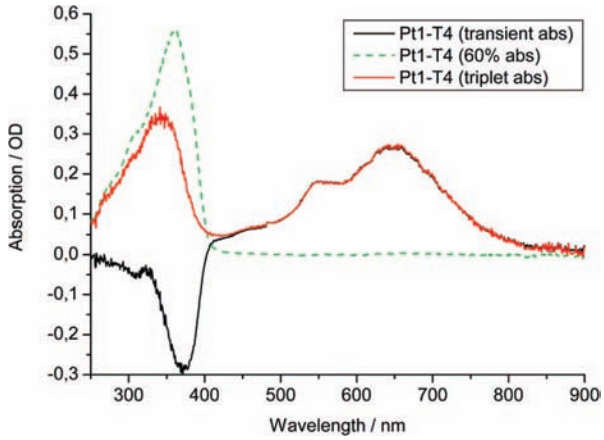

Figure 9. Transient absorption spectrum of **Pt1-T4** and 60% absorption spectrum (dashed). The true triplet state absorption spectrum (red) is the sum of the other two.

the initially excited molecules are transferred to the triplet manifold. Since the transient spectrum is measured with a reference where 100% of the molecules are in the ground state, a ground-state depletion peak will appear in the spectrum. The degree of ground-state depletion was estimated by adding a fraction of the ground-state absorption spectrum to the transient spectrum as shown in Figure 9 for **Pt1-T4** in such a way that the structure of the depletion part of the spectrum vanishes; see section 2.5.

The delay between the pump and probe pulse was set to 5 μs. In Figure 9, for **Pt1-T4**, 60% ground-state absorption was added to the transient absorption spectrum. That is, 60% of the molecules are excited from the ground-state by the pump light at the time when the transient absorption measurement is taken. Figure 9 also shows that the ground-state depletion and the absorption spectrum do not overlap at short wavelengths, $\leq$400 nm, and therefore an additional triplet−triplet absorption peak is observed in the UV region. Since the triplet state of **Pt1-T4** predominantly is localized to one of the acetylide ligands after 5 μs ("**T4** side" of **Pt1-T4**), the other acetylide ligand remains mainly in the ground-state configuration. Thus, the triplet absorption in the UV region is assigned to an $S_0 \rightarrow S_1$ type of absorption, localized to the "**Pt1** side". This is in agreement with the maximum of this absorption being similar in energy (blue-shifted approximately 15 nm) to the strong $S_0 \rightarrow S_1$ absorption of **Pt1** and **Pt1-G1**. Recently, similar observations have been made for a series of platinum-acetylide oligomers,[53] and as found by Cooper et al.[29,30] the blue-shift obtained for a "half-Pt-molecule" ($Cl-Pt(PBu_3)_2$-CC-C_6H_4−CC-C_6H_5) is only 11 nm compared to a similar molecule symmetrically substituted with two identical ligands.

The transient absorption spectra of the thiophenes **T3**, **T4**, **T6**, **T7** and of **Pt3**,[35] as well as of triazoles **Z1** and **Z3**[37] were also recorded. The absorption peaks in the visible region and the extinction coefficients of these compounds are listed in Table 2. We note that the peak wavelength of the triplet absorption increases in the order **T7** < **T3** < **T4**, that is, in the opposite order to the ground-state absorption. Hence, the compound that displays the largest red-shift (**T4**) has the thiophene unit as the terminal ring, in contrast to the case for ground-state absorption where **T7**, which has the thiophene group closest to the Pt atom, shows the largest red-shift.[35] However, **T6** is the most red-shifted of all five compounds in both cases. The triplet−triplet absorption peak of **Pt3** is found to be more red-shifted than **T4** (but less than **T6**). This means that the introduction of the thiophene ring results in a blue-shift of the triplet−triplet absorption and an increased blue-shift as this ring is placed closer to the Pt atom.

The **Z3** compound showed similar triplet absorption as **Pt1-G1**. It has a longer triplet decay lifetime ($\tau_{phos} = 0.31$ ms) than **Pt1-G1** and a slightly stronger estimated absorption depletion and therefore has an apparently larger extinction coefficient. **Z1** on the other hand shows only weak transient absorption after 5−10 μs, probably due to its significantly shorter triplet state lifetime of 0.59 μs as determined by the phosphorescence decay.

Our results of the triplet−triplet state absorption of **Pt1-G1** and **Pt3** are similar to those found by McKay et al.[23] and Cooper et al.[30,55] for **Pt1** and **Pt3**, with absorption peaks at 590 and 650 nm, respectively. Our values of the extinction coefficients at the absorption maxima are however somewhat lower than those found by Cooper et al.[30] The difference in pulse length and time delay in the two setups may have an effect on the results. In their experiments, a 30-ps pulse duration and a 105-ps time delay were used while we applied a 5-μs pulse length and 5−10-μs time delays.

The appearance of transient triplet absorption spectra can be used to deduce the OPL performance. OPL measurements of the **Pt1**-type, **T**-series, and **Z**-series have previously been published by our research group,[8,36,37] and additional data are given in a companion paper.[35] OPL measurements were in most cases measured at 532 nm using 5-ns pulses from a 10 Hz Nd:YAG laser in a f/5 setup. The process of nonlinear absorption utilizing the triplet states is complex. In the simplest model the linear absorption, ISC efficiency, triplet absorption, and triplet lifetime must be taken into account. In general, the longer molecules (**Pt3**-like) shows slightly better OPL than the shorter (**Pt1**, **Pt1-G1**).[35] However, the photophysical properties are not found to differ significantly. One reason for better OPL of **Pt3** may be the somewhat larger triplet absorption coefficient for this compound. In the case of **Z3**, the better OPL performance compared to **Pt1-G1**[37] can be explained by a combination of larger ground-state absorption, longer triplet lifetime, and increased triplet absorption. The same may be valid for the **T6** molecule compared with the others in the **T**-series and with **Pt3**. The inferior OPL performance of the **Z1** molecule can be explained by the same token from a decrease in the same three parameters. Although the trend is clear for some of the molecules, no further conclusions can be obtained for the other compounds. We also note that nonlinear scattering may contribute to the OPL performance, and therefore makes the situation more complex.

4. Conclusions

The absorption, ISC, phosphorescence, and transient absorption properties of a series of platinum(II) acetylide chromophores containing thiophene and triazole groups, and with different substituents, were investigated. Four new Pt(II) acetylides were also investigated for their photophysical properties. The new compounds show strong absorption and bright phosphorescence in oxygen-evacuated samples, except for the compound with bithienyl groups, which showed only weak phosphorescence but still some transient absorption. All other molecules show strong triplet state absorption over the whole visible region, in a range from 20% to 70% of the ground-state absorption strength. The data for the compound with two different arylalkynyl ligands suggest fast energy transfer from a localized triplet at the shorter ligand to the longer one, which enhances both the lifetime and triplet absorption of the longer ligand.

Acknowledgment. This work has been supported by the "Swedish Defence Nano Technology Programme" managed by the Swedish Defence Research Agency (FOI). M.L. also acknowledges a grant from the Norwegian Research Council within the NanoMat program (Contract No. 163529/S10).

References and Notes

(1) Kingsborough, P. R.; Swager, T. M. *Prog. Inorg. Chem.* **1999**, *48*, 123.
(2) Skotheim, T. A.; Elsenbaumer, R. L.; Raynolds, J. R. *Handbook of Conducting Polymers*, 2nd ed.; Marcel Dekker: New York, 1998.
(3) Gunder, P. *Nonlinear Optical Effects and Materials*; Springer: New York, 2000.
(4) Whittall, I. R.; McDonagh, A. M.; Humphrey, M. G.; Samoc, M. *Adv. Organomet. Chem.* **1998**, *42*, 291.
(5) Tessler, N.; Damon, G. J.; Friend, R. H. *Nature* **1996**, *382*, 695.
(6) Fortrie, R.; Anémian, R.; Stephan, O.; Mulatier, J.-C.; Baldeck, P. L.; Andraud, C.; Chermette, H. *J. Phys. Chem. C* **2007**, *111*, 2270.
(7) Staromlynska, J.; McKay, T. J.; Wilson, P. *J. Appl. Phys.* **2000**, *88*, 1726.
(8) Vestberg, R.; Westlund, R.; Eriksson, A.; Lopes, C.; Carlsson, M.; Eliasson, B.; Glimsdal, E.; Lindgren, M.; Malmström, E. *Macromolecules* **2006**, *39*, 2238.
(9) Girardot, C.; Cao, B.; Mulatier, J.-C.; Baldeck, P. L.; Chauvin, J.; Riehl, D.; Delarie, J. A.; Andraud, C.; Lemercier, G. *ChemPhysChem* **2008**, *9*, 1531.
(10) Nilsson, K. P. R.; Åslund, A.; Berg, I.; Nyström, S.; Konradsson, P.; Herland, A.; Inganäs, O.; Stabo-Eeg, F.; Lindgren, M.; Westermark, G. T.; Lannfelt, L.; Nilsson, L. N. G.; Hammarström, P. *Chem. Biol.* **2007**, *2*, 553.
(11) D'Aléo, A.; Pompidor, G.; Elena, B.; Vicat, J.; Baldeck, P. L.; Toupet, L.; Kahn, R.; Andraud, C.; Maury, O. *ChemPhysChem* **2007**, *8*, 2125.
(12) Nilsson, K. P. R.; Hammarström, P.; Ahlgren, F.; Herland, A.; Schnell, E. A.; Lindgren, M.; Westermark, G. T.; Inganäs, O. *ChemBioChem* **2006**, *7*, 1096.
(13) Cifuentes, M. P.; Humphrey, M. G. *J. Organomet. Chem.* **2004**, *689*, 3968.
(14) Powel, C. E.; Humphrey, M. G. *Coord. Chem. Rev.* **2004**, *248*, 725.
(15) Vlcek, A., Jr. *Coord. Chem. Rev.* **2000**, *200*−*202*, 933.
(16) Sun, S.-S.; Lees, A. J. *Coord. Chem. Rev.* **2002**, *230*, 171.
(17) Whittall, I. R.; McDonagh, A. M.; Humphrey, M. G.; Samoc, M. *Adv. Organomet. Chem.* **1999**, *43*, 349.
(18) Nalwa, H. S. *Appl. Organomet. Chem.* **1991**, *5*, 349.
(19) Haskins-Glusac, K.; Ghiviriga, I.; Abboud, K. A.; Schanze, K. S. *J. Phys. Chem. B* **2004**, *108*, 4969.
(20) Masai, H.; Sonogashira, K.; Hagihara, N. *Bull. Chem. Soc. Jpn.* **1971**, *44*, 2226.
(21) Staromlynska, J.; McKay, T. J.; Bolger, J. A.; Davy, J. R. *J. Opt. Soc. Am. B* **1998**, *15*, 1731.
(22) McKay, T. J.; Bolger, J. A.; Staromlynska, J.; Davy, J. R. *J. Chem. Phys.* **1998**, *108*, 5537.
(23) McKay, T. J.; Staromlynska, J.; Davy, J. R.; Bolger, J. A. *J. Opt. Soc. Am. B* **2001**, *18*, 358.
(24) Rogers, J. E.; Cooper, T. M.; Fleitz, P. A.; Glass, D. J.; McLean, D. G. *J. Phys. Chem. A* **2002**, *106*, 10108.
(25) Cooper, T. M.; Blaudeau, J.-P.; Hall, B. C.; Rogers, J. E.; McLean, D. L.; Liu, Y.; Toscano, J. P. *Chem. Phys. Lett.* **2004**, *400*, 239.
(26) Cooper, T. M.; McLean, D. L.; Rogers, J. E. *Chem. Phys. Lett.* **2001**, *349*, 31.
(27) Cooper, T. M.; Hall, B. C.; McLean, D. L.; Rogers, J. E.; Burke, A. R.; Turnbull, K.; Weisner, A.; Fratini, A.; Liu, Y.; Schanze, K. S. *J. Phys. Chem. A* **2005**, *109*, 999.
(28) Rogers, J. E.; Hall, B. C.; Hufnagle, D. C.; Slagle, J. E.; Ault, A. P.; McLean, D. G.; Fleitz, P. A.; Cooper, T. M. *J. Chem. Phys.* **2005**, *122*, 214708.
(29) Cooper, T. M.; Krein, D. M.; Burke, A. R.; McLean, D. L.; Rogers, J. E.; Slagle, J. E.; Fleitz, P. A. *J. Phys. Chem. A* **2006**, *110*, 4369.
(30) Cooper, T. M.; Krein, D. M.; Burke, A. R.; McLean, D. L.; Rogers, J. E.; Slagle, J. E. *J. Phys. Chem. A* **2006**, *110*, 13370.
(31) Lindgren, M.; Minaev, B.; Glimsdal, E.; Vestberg, R.; Westlund, R.; Malmström, E. *J. Lumin.* **2007**, *124*, 302.
(32) Baev, A.; Norman, P.; Henriksson, J.; Ågren, H. *J. Phys. Chem. B* **2006**, *110*, 20912.
(33) Lind, P.; Boström, D.; Carlsson, M.; Glimsdal, E.; Lindgren, M.; Lopes, C.; Eliasson, B. *J. Phys. Chem. A* **2007**, *111*, 1598.
(34) Glimsdal, E.; Carlsson, M.; Eliasson, B.; Minaev, B.; Lindgren, M. *J. Phys. Chem. A* **2007**, *111*, 244.
(35) Carlsson, M.; Glimsdal, E.; Lindgren, M.; Lopes, C.; Eliasson, B. Synthesis of diacetylide Platinum (II) diphosphine complexes and nonlinear absorption of light. To be submitted.
(36) Glimsdal, E.; Carlsson, M.; Eliasson, B.; Westlund, R.; Lindgren, M. *Proc. SPIE* **2007**, *6740*, 67400M.
(37) Westlund, R.; Glimsdal, E.; Vestberg, R.; Hawker, C.; Lindgren, M.; Eriksson, A.; Lopes, C.; Malmström, E. *J. Mater. Chem.* **2008**, *18*, 166.
(38) Westlund, R.; Lopes, C.; Rodgers, T.; Saito, Y.; Kawata, S.; Glimsdal, E.; Lindgren, M.; Malmström, E. *Adv. Mater. Chem.* **2008**, *18*, 1939.
(39) Merkushev, E. B.; Simakhina, N. D.; Koveshnikova, G. M. *Synthesis* **1980**, 486.
(40) Kauffman, G. B.; Teter, L. A. *Inorg. Synth.* **1963**, *7*, 245.
(41) Lavastre, O.; Cabioch, S.; Dixneuf, P. H.; Vohlidal, J. *Tetrahedron* **1997**, *53*, 7595.
(42) Carlsson, M. *Synthesis and optical characterization of optical power limiting platinum(II) acetylides*; PhD Thesis; Umeå University; Umeå, 2007.
(43) Sasaki, T.; Tour, J. M. *Tetrahedron Lett.* **2007**, *48*, 5821.
(44) Dirk, S. M.; Price, D. W.; Chanteau, S.; Kosynkin, D. V.; Tour, J. M. *Tetrahedron* **2001**, *57*, 5109.
(45) Curtis, R. F.; Phillips, G. T. *J. Chem. Soc.* **1965**, 5134.
(46) Epstein, W. W.; Gerike, P.; Horton, W. J. *Tetrahedron Lett.* **1965**, 3991.
(47) Atkinson, R. E.; Curtis, R. F.; Phillips, G. T. *J. Chem. Soc.* **1965**, 7109.
(48) Patrick, T. B.; Honegger, J. L. *J. Org. Chem.* **1974**, *39*, 3791.
(49) Williams, A. T. R.; Winfield, S. A.; Miller, J. N. *Analyst* **1983**, *108*, 1067.
(50) A Guide to Recording Fluorescence Quantum Yields, HORIBA Jobin Yvon Inc.
(51) Emmert, L. A.; Choi, W.; Marshall, J. A.; Yang, J.; Meyer, L. A.; Brozik, J. A. *J. Phys. Chem. A* **2003**, *107*, 11340–11346.
(52) Batista, E. R.; Martin, R. L. *J. Phys. Chem. A* **2005**, *109*, 9856–9859.
(53) Glusac, K.; Köse, M. E.; Jiang, H.; Schanze, K. S. *J. Phys. Chem B* **2007**, *111*, 929.
(54) Minaev, B.; Jansson, E.; Lindgren, M. *J. Chem. Phys.* **2006**, *125*, 094306.
(55) Cooper, T. M.; Hall, B. C.; Burke, A. R.; Rogers, J. E.; McLean, D. G.; Slagle, J. E.; Fleitz, P. A. *Chem. Mater.* **2004**, *16*, 3215.

JP8083277